Visualization of the Hexagonal Lattice in the Erythrocyte Membrane Skeleton

Shih-Chun Liu, Laura H. Derick, and Jiri Palek

Department of Biomedical Research and Medicine, Division of Hematology/Oncology, St. Elizabeth's Hospital of Boston, Tufts University School of Medicine, Boston, Massachusetts 02135

Abstract. The isolated membrane skeleton of human erythrocytes was studied by high resolution negative staining electron microscopy. When the skeletal meshwork is spread onto a thin carbon film, clear images of a primarily hexagonal lattice of junctional F-actin complexes crosslinked by spectrin filaments are obtained. The regularly ordered network extends over the entire membrane skeleton. Some of the junctional complexes are arranged in the form of pentagons and septagons, ~3 and 8%, respectively. At least five forms of spectrin crosslinks are detected in the spread skeleton including (*a*) a single spectrin tetramer linking two junctional complexes, (*b*) three-armed Y-shaped spectrin molecules linking three junctional complexes, (*c*) three-armed spectrin molecules connecting two junctional complexes with two arms bound to one complex and the third arm bound to the adjacent complex, (*d*) double spectrin filaments linking two junctional complexes, and (*e*) four-armed spectrin molecules linking two junctional complexes. Of these, the crosslinks of single spectrin tetramers and three-armed molecules are the most abundant and represent 84 and 11% of the total crosslinks, respectively. These observations are compatible with the presence of spectrin tetramers and oligomers in the erythrocyte membrane skeleton. Globular structures (9–12 nm in diameter) are attached to the majority of the spectrin tetramers or higher order oligomer-like molecules, ~80 nm from the distal ends of the spectrin tetramers. These globular structures are ankyrin- or ankyrin/band 3-containing complexes, since they are absent when ankyrin and residual band 3 are extracted from the skeleton under hypertonic conditions.

THE inner side of the mammalian erythrocyte membrane is laminated by a protein network principally composed of spectrin, actin, band 4.1, and band 4.9 (see 2, 6, 25, 26 for reviews). Many intermolecular associations of these membrane skeletal proteins are now relatively well understood. Spectrin, the major protein constituent of the membrane skeleton, accounts for ~75% of the skeletal mass. In the αβ dimeric form (α-chain, 240,000 daltons; β-chain, 220,000 daltons) in solution, spectrin appears as an elongated, highly flexible, double stranded molecule ~100 nm long (36). Head to head association of two spectrin dimers forms a tetramer that is about twice as long.

In solution, spectrin dimers can undergo reversible self-association to form tetramers (45) and higher order oligomers (28). In the membrane, spectrin tetramers and medium-sized oligomers are thought to be the prominent species, accounting for 45–55% and 25-35% of spectrin, respectively (21). Among these medium sized spectrin oligomers, spectrin hexamers are the most abundant, representing ~14% of the total spectrin.

Biochemical evidence has indicated that the actin in the membrane skeleton is in the filamentous form (for review see reference 6). Based on the estimated number of actin molecules per cell and on the titer of cytochalasin binding sites, which are at the filament ends in the membrane, each actin filament may contain 10–18 monomers (4, 19, 31). However, the presence of much longer filaments of actin has been suggested by others (1).

In the absence of band 4.1, spectrin binds weakly to F-actin (3, 7, 8, 44). However, in the ternary system containing F-actin, spectrin dimer, and band 4.1, spectrin binds strongly to F-actin, resulting in F-actin filaments decorated randomly with convoluted spectrin dimers (7, 8, 9, 16, 44). An extended network can be formed if the bifunctional spectrin tetramer, instead of spectrin dimer, is included in the ternary system (9, 44). Each spectrin tetramer contains two binding sites, one at either end, for band 4.1 (43) and for F-actin (9).

Earlier electron microscopic studies of the membrane skeleton were complicated by the high density of the native skeleton. Using various techniques of specimen preparation, such as negative staining (33, 39, 47), thin sectioning (40, 41), shadowing (30), rapid freezing (12, 27), and scanning electron microscopy (17), these studies revealed only a filamentous weblike structure containing a variety of poorly defined elements of various sizes. Recently, however, the resolution was drastically improved when the membrane skeleton was either fragmented or artificially spread and then examined by negative staining electron microscopy.

Shen, Josephs, and Steck succeeded in obtaining images of membrane skeletons and their fragments at high resolution (34, 35). The fragmented skeleton, generated under conditions that destroy the self-association of spectrin but preserve the spectrin-actin-4.1 interaction, contains two basic structural elements: (*a*) 7–8-nm-thick filaments, representing short F-actin (i.e., actin protofilaments) and (*b*) thin and convoluted filaments of spectrin projecting from these actin protofilaments. Recently, an electron microscopic study by Byers and Branton (5) of the spread membrane skeleton derived from the intact cell showed clear images of the intact skeletal network with thick filaments of short F-actin with five or six spectrin tetramers joining at each short F-actin junction, suggesting the possibility of a regular long range order in the skeleton. In addition, both groups detected globular structures (78 ± 7 nm in diameter) attached to spectrin filaments at the site very close to the known binding site for ankyrin (5, 35). However, it remains uncertain whether or not (*a*) these skeletal components are assembled into a specific lattice of long range order, (*b*) spectrin oligomers can also cross-link short F-actin in the skeleton, and (*c*) the spectrin filaments can cross over each other to bind to short F-actin.

In the present study, we have improved the spreading of the skeleton on thin carbon film and examined the skeleton by high resolution negative staining electron microscopy. The proteins in the skeletal network are connected in a primarily hexagonal array. Junctional complexes at the center and at the six corners of each hexagon are linked to the adjacent complexes by filaments resembling spectrin tetramers and medium-sized oligomers. Less frequently, junctional complexes are arranged in the pentagonal and septagonal forms. In addition, globular ankyrin-containing complexes that are attached to the spectrin filaments could be removed from the skeleton under hypertonic conditions. These data have been presented in preliminary form (24).

Materials and Methods

Membrane Skeleton Preparation

Venous blood from normal individuals was collected in sterile tubes containing citrate-phosphate-dextrose or acid-citrate-dextrose as anticoagulant and analyzed within a week. Ghost membranes were prepared by the method of Dodge et al. (11) with 5 mM NaPi (pH 7.4). Freshly prepared ghosts (1 mg protein/ml) were incubated on ice for 60 min in 4 vol of 5 mM NaPi (pH 7.4) containing 2.5% (wt/vol) Triton X-100. The mixture was layered on top of a discontinuous gradient of 10 and 60% (wt/vol) sucrose containing 0.1 mM NaPi (pH 7.0) and 0.5 mM dithiothreitol and centrifuged at 100,000 *g* for 15 min in a swinging bucket rotor. The intact skeletons were collected from the 10%/60% sucrose interface essentially as previously described (32–34). To remove bands 2.1 and 3 from the membrane skeleton, NaCl (final concentration 1.5 M) was incorporated into the sucrose solutions used for centrifugation. The isolated membrane skeletons were routinely checked for size and shape by means of a phase contrast light microscope attached to a Newvicon camera (23).

To induce a partial dissociation of spectrin tetramers into dimers in the membrane, ghosts from normal erythrocytes were incubated hypotonically at 37°C for 15 min in 5 mM NaPi (pH 7.4) containing 15 mM NaCl, 0.1 mM phenylmethyl sulfonyl fluoride, and 1 mM EDTA. Subsequently these ghosts were washed hypotonically at 4°C and subjected to Triton X-100 extraction and sucrose density gradient centrifugation as described above. An aliquot of ghosts was subjected to low-salt extraction and analysis of the spectrin species in the extract by nondenaturing gel electrophoresis as described previously (20).

Preparation of Carbon-coated Copper Grids

To obtain high contrast images, a thin film of carbon was used to support the specimen. This thin carbon film (~0.6 nm thick) was produced by depositing a small amount of carbon on a freshly cleaved mica surface in a freeze-etch unit (Balzers BAF 400D; Balzers AG, Liechtenstein). The thickness of the carbon film was calculated from the frequency change detected with a quartz crystal monitor in the Balzer unit (42). The thin film was carefully floated onto distilled water in a Smith grid coating trough (Ladd Research Industries, Burlington, VT) (38) and lowered onto bare 1,000-mesh copper grids or holey Formvar grids similar to that used by Craig et al. (10). The grids coated with thin carbon were subjected to glow discharge with a vacuum evaporator just before use for specimen preparation. The holey Formvar grids were prepared on copper grids as follows: glycerol (50%; 1 ml) was added dropwise to a solution of 0.5% Formvar in ethylene dichloride. The mixture was sonicated with a probe sonicator until hot (2 min). Glass slides were dipped into the solution, allowed to dry, and then the holey Formvar film was floated onto the water. The holey film was lowered onto the grids using the grid coating trough, allowed to dry, and then placed on a bed of methanol-saturated filter paper for 5–10 min to remove remaining glycerol drops and to etch pseudo holes.

Negative Staining Electron Microscopy

To prepare a specimen for electron microscopy, an aliquot of membrane skeletons in sucrose was diluted with 9 vol of 0.1 mM NaPi (pH 7.0) buffer, applied to a carbon-coated grid, and allowed to adsorb to the film for 10 min at 4°C. The grid was then rinsed with 0.1 mM NaPi (pH 7.0) buffer, fixed with 2.5% glutaraldehyde in 0.1 mM NaPi (pH 7.0) at 25°C for 10 min, and negatively stained with 1% uranyl acetate solution for 1–2 min. The excess solution was drawn into filter paper and grids were air dried. Specimens were examined in a Jeol JEM-100 S electron microscope with an accelerating voltage of 60 kV.

Gel Electrophoresis

Electrophoresis under nondenaturing conditions was carried out in an agarose (0.3%)-polyacrylamide (2.5%) composite gel at 4°C as described previously (20). SDS-polyacrylamide (5.6%) gel electrophoresis (SDS PAGE) was performed as described (13).

Results

The Normal Membrane Skeleton Consists of a Hexagonal Lattice

Fig. 1 *a* shows a negatively stained membrane skeleton with a clear image of a large area of spread meshwork at the marginal region of the skeleton, which was partially disrupted as a result of the drying process during specimen preparation, tearing off the upper layer while exposing the bottom layer of the skeleton. It is readily apparent that this extended skeleton is organized into a highly ordered lattice. A closer inspection at higher magnification of a well preserved area revealed that the skeletal proteins are connected in a primarily hexagonal array. Junctional complexes (9–16 nm thick, 38–50 nm long; presumably representing short F-actin and the associated proteins) are located at the center and six corners of the hexagon (Fig. 1, *b* and *c*). These junctional complexes are cross-linked to their adjacent complexes by long flexible filaments resembling spectrin tetramers and higher order oligomers. As previously observed by others, these spectrin filaments often have globular structures (9–12 nm) attached to their ankyrin binding site(s), that is, 80 nm from the distal end of the spectrin tetramers. These 9–12-nm globules probably represent ankyrin and its associated band 3 (see below). In addition to the hexagonal array, we also found a smaller number of skeletal subunits in the pentagonal and septagonal forms (Fig. 2) representing ~3 and 8%,

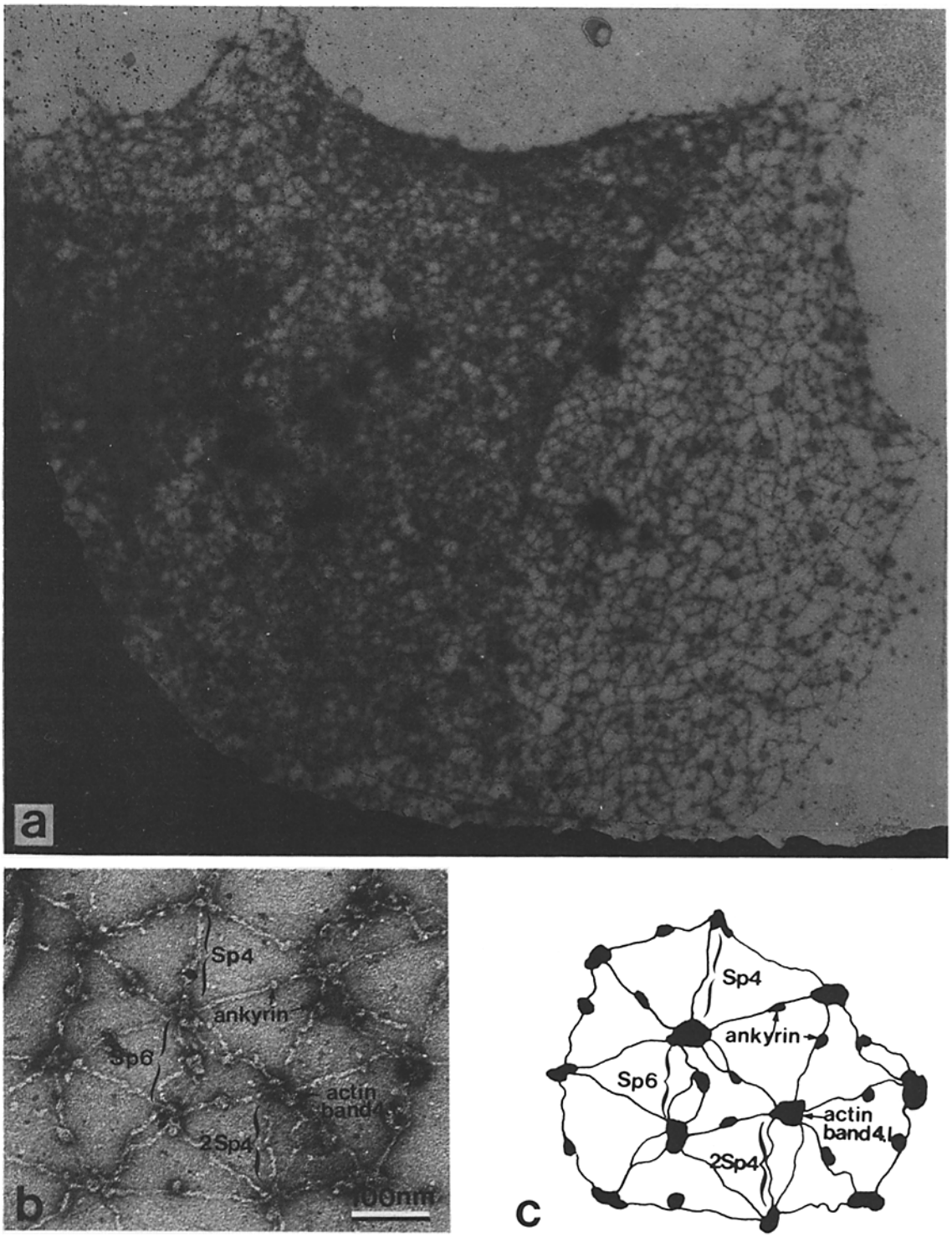

Figure 1. Spread membrane skeleton examined by negative-staining electron microscopy. Membrane skeletons derived from Triton-treated (2.0%) normal red cell ghosts were isolated by sucrose density gradient centrifugation under hypotonic conditions. The skeletons were applied to thin carbon-coated grids, fixed with glutaraldehyde, stained with uranyl acetate, air dried, and examined by transmission electron microscopy. (*a*) A large area of a spread meshwork is shown revealing the marginal region of the exposed bottom layer of the skeleton. (*b*) A higher magnification of the spread meshwork reveals the hexagonal lattice of junctional complexes, presumably containing short F-actin and band 4.1, cross-linked by spectrin tetramers (*Sp4*), three-armed spectrin molecules (*Sp6*), and double spectrin filaments (*2 Sp4*). Globular structures of ankyrin (or ankyrin-containing complexes) are attached to spectrin filaments at the ankyrin-binding site, i.e., 80 nm from the distal end of spectrin. (*c*) A tentative assignment of these structural elements is given in the schematic diagram.

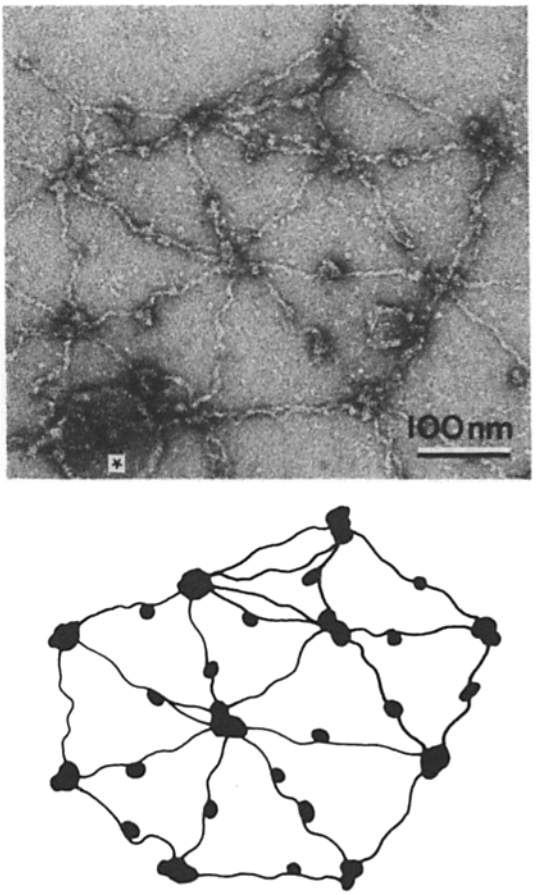

Figure 2. Septagonal and pentagonal subunits in the spread membrane skeleton. A septagonal subunit is shown in the lower left-hand corner, whereas an adjacent pentagonal subunit is shown in the upper right-hand corner. A dense region of residual membrane material is indicated by an asterisk at the lower left hand corner.

respectively (n = 163). Fig. 3 shows, in a different preparation, a large area of the spread skeleton at high magnification. Many subunits in the spread skeleton do not contain all the spectrin cross-links between adjacent junctional complexes, presumably due to partial disruption occurring during specimen preparation. However, we can not exclude the possibility that some of the missing spectrin cross-links may already be absent in the native membrane.

The membrane skeletons shown in Figs. 1–3 were examined on a very thin carbon film to obtain high contrast. The thin carbon film is supported and strengthened by a fine 1,000-mesh grid or a holey Formvar coated grid. The advantage of using a continuous thin carbon film instead of a fenestrated carbon film (34, 35) to support the membrane skeleton is that the skeleton can be artificially spread during specimen preparation due to a contraction of skeletal material toward the center of the specimen while the skeletal margin is still firmly attached to the thin carbon film on the copper grid. Fig. 4 shows a spread skeleton with an asymmetric lattice due to the uneven stretching of the network during specimen preparation. In some areas the cross-bridges were stretched into straight filaments in one axis to ~200 nm, which is the contour length of a spectrin tetramer. In other axes of the same areas, spectrin cross-bridges between adjacent junctional complexes are more convoluted and relaxed. It is possible that this spring-like flexibility of spectrin is important in facilitating the deformability of the intact erythrocyte. Fig. 5 shows a spread region of the double layered intact skeleton, indicating that stretched spectrin filaments of the bottom layer were crossed over by spectrin filaments of the upper layer of the skeleton. This type of image helps us to distinguish between the irregular polygonal images generated from skeleton overlap and the pentagons, hexagons, and septagons observed on the spread monolayered skeleton (Figs. 1–3). In addition, we often detected a progressive decrease in the stretching of the network from the marginal region to the center of the skeleton preparation. It appears that the meshwork generated by spreading the isolated skeleton, as compared with that obtained from intact cells (5), produces a much larger area of a continuous lattice for detailed visualization. The ultrastructural information obtained from the isolated skeleton may be correlated directly with the skeletal protein composition and facilitate the molecular assignment of some of the structural elements.

Large areas of the hexagonal lattice in the spread membrane skeleton are detected reproducibly in different skeleton preparations. The inclusion of glutaraldehyde fixation in the skeleton preparation for electron microscopic examination is important for the preservation of the skeletal protein connections. It seems to reduce the degree of partial disruption of the network structure, especially at the marginal region of the spread skeleton during specimen preparation. However, a hexagonal array of the proteins is still detectable without glutaraldehyde fixation (data not shown). In addition, preparation of erythrocyte skeletons at different hypotonic salt concentrations (e.g., 0–20 mM NaCl) or temperatures (e.g., 0–25°C) does not change the ultrastructure of the spread skeleton (data not shown).

Spectrin Cross-links in the Spread Membrane Skeleton

Although the 200-nm spectrin tetramers appear to be the most prominent species of spectrin to cross-link the junctional complexes of actin, we detected a significant amount of spectrin (16% of total, n = 341) in several different forms including (*a*) three-armed, Y-shaped spectrin molecules linking three junctional complexes (Fig. 6, *a* and *b*), (*b*) three-armed spectrin molecules with two arms bound to a junctional complex and the third arm bound to the adjacent complex (Fig. 1 *b*), (*c*) two separated spectrin filaments linking two junctional complexes (Fig. 1 *b*), and (*d*) four-armed spectrin molecules linking two junctional complexes (Fig. 6 *c*). Among these the three-armed spectrin molecules are the most abundant, representing ~11% of the total cross-links. These observations are compatible with the presence of spectrin tetramers and possibly other medium-sized oligomers in the erythrocyte membrane, as previously indicated by biochemical analysis (21, 28).

At the present time, however, the identification of different oligomeric species of spectrin in the spread skeleton is still premature. These oligomeric-like images may be generated from spectrin tetramers by a splitting of the α- and β-chains of one or both of the dimeric subunits or alternatively by breakage and rearrangement of spectrin tetramers in situ or during specimen preparation.

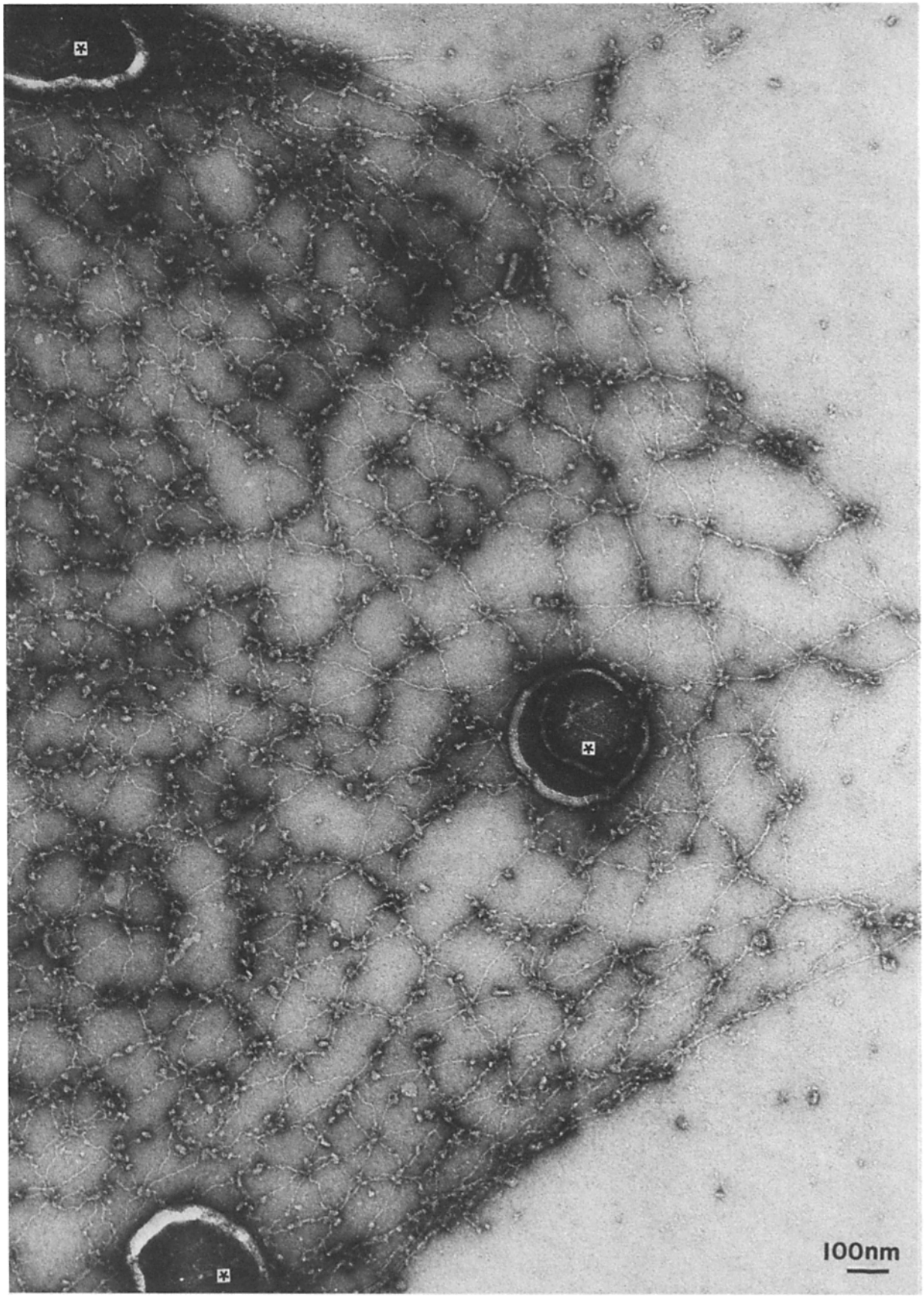

Figure 3. Spread membrane skeleton. A large area of the spread skeleton at high magnification is shown. Dense regions labeled by asterisks are residual membrane components not extracted by Triton X-100.

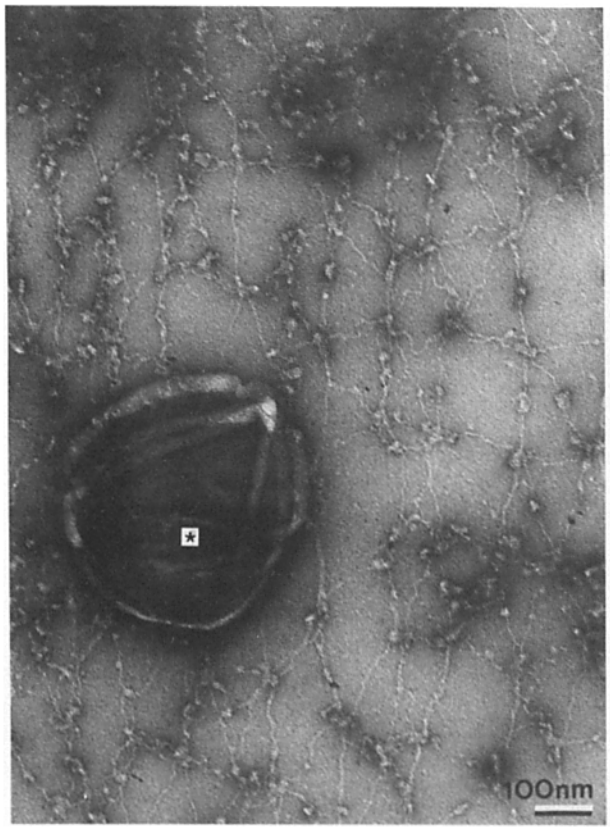

Figure 4. Asymmetric stretching of the membrane skeleton. The uneven spreading of the skeleton shows more stretching in the vertical as compared with the horizontal direction. Continuous fibers are aligned in the vertical direction and are formed by the alternative linkings of short F-actin and 200-nm spectrin tetramers. A dense region labeled by an asterisk represents residual material not extracted by Triton X-100.

Ultrastructure of Spectrin and Spectrin-Actin-Band 4.1 Complexes in Solution

To identify the structural elements observed in the intact spread skeleton, we examined spectrin and spectrin-actin-band 4.1 complexes derived from the 0°C low-salt membrane extract (21) using the same negative staining electron microscopic technique. The results are shown in Fig. 7 and demonstrate that: (*a*) the morphology of isolated spectrin tetramers is similar to that of the elongated thin filaments (200 nm long) in the spread meshwork, (*b*) no splitting of α- and β-chains was evident in the negatively stained spectrin dimers or tetramers, and (*c*) the spectrin-actin-band 4.1 complexes contained a structure similar to the junctional complexes detected in the skeleton, and some of these complexes were still cross-linked by spectrin filaments.

Ultrastructure of Membrane Skeletons Stripped of Ankyrin and Band 3

Triton shells prepared in hypotonic buffer (5 mM NaPi, pH 7.4) with 2.5% Triton X-100 retained all the skeletal proteins, spectrin, actin, band 4.1, and band 4.9 but only part of the ankyrin (60–80%) and band 3 (10–20%), as analyzed by SDS PAGE (Fig. 8 *a*). Most of the residual ankyrin and band 3 of the Triton shell could be removed by sedimentation through a sucrose layer containing 1.5 M NaCl at 4°C (Fig. 8 *a*). As previously shown (32, 34), these ankyrin- and band 3-stripped membrane skeletons shrank in 1.5 M NaCl to 2–3 μm in diameter, but after reincubation in low ionic strength buffer (0.1 mM NaPi, pH 7.0), they expanded to 5–8 μm in diameter (data not shown). Electron microscopic studies of these reswollen membrane skeletons, stripped of ankyrin and band 3, showed that the network was somewhat aggregated but still contained recognizable junctional complexes that were mostly linked by bare cross-bridges, i.e., spectrin fila-

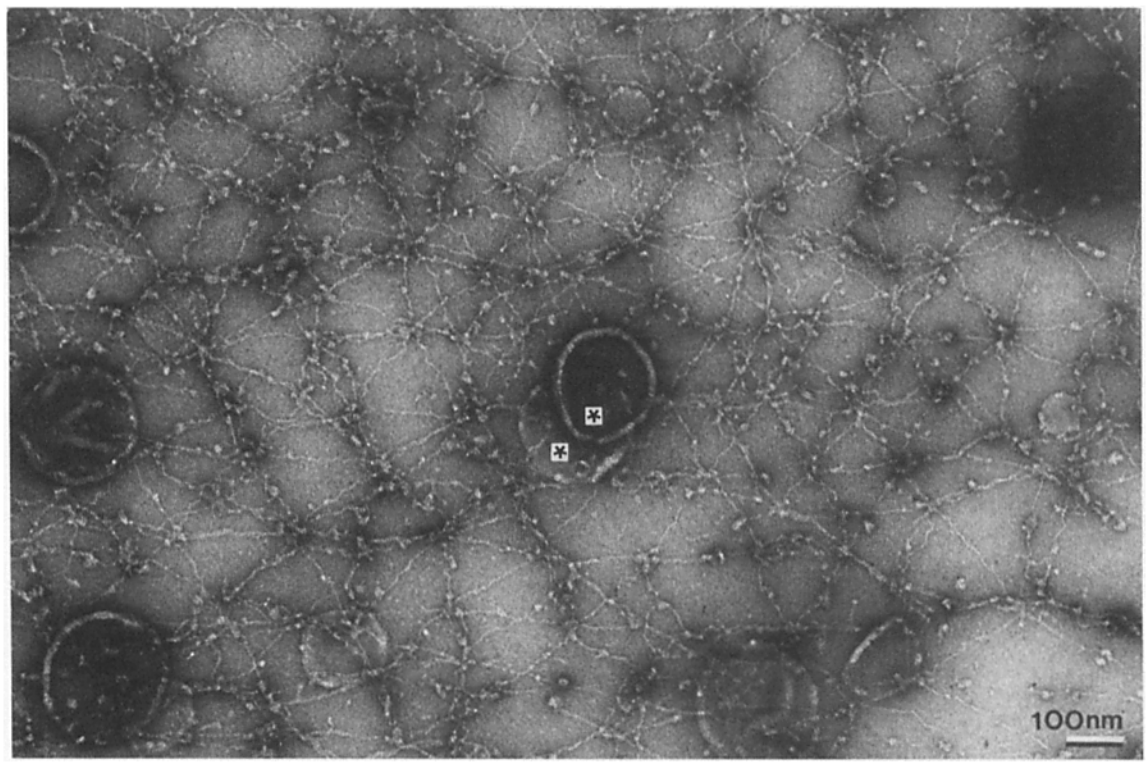

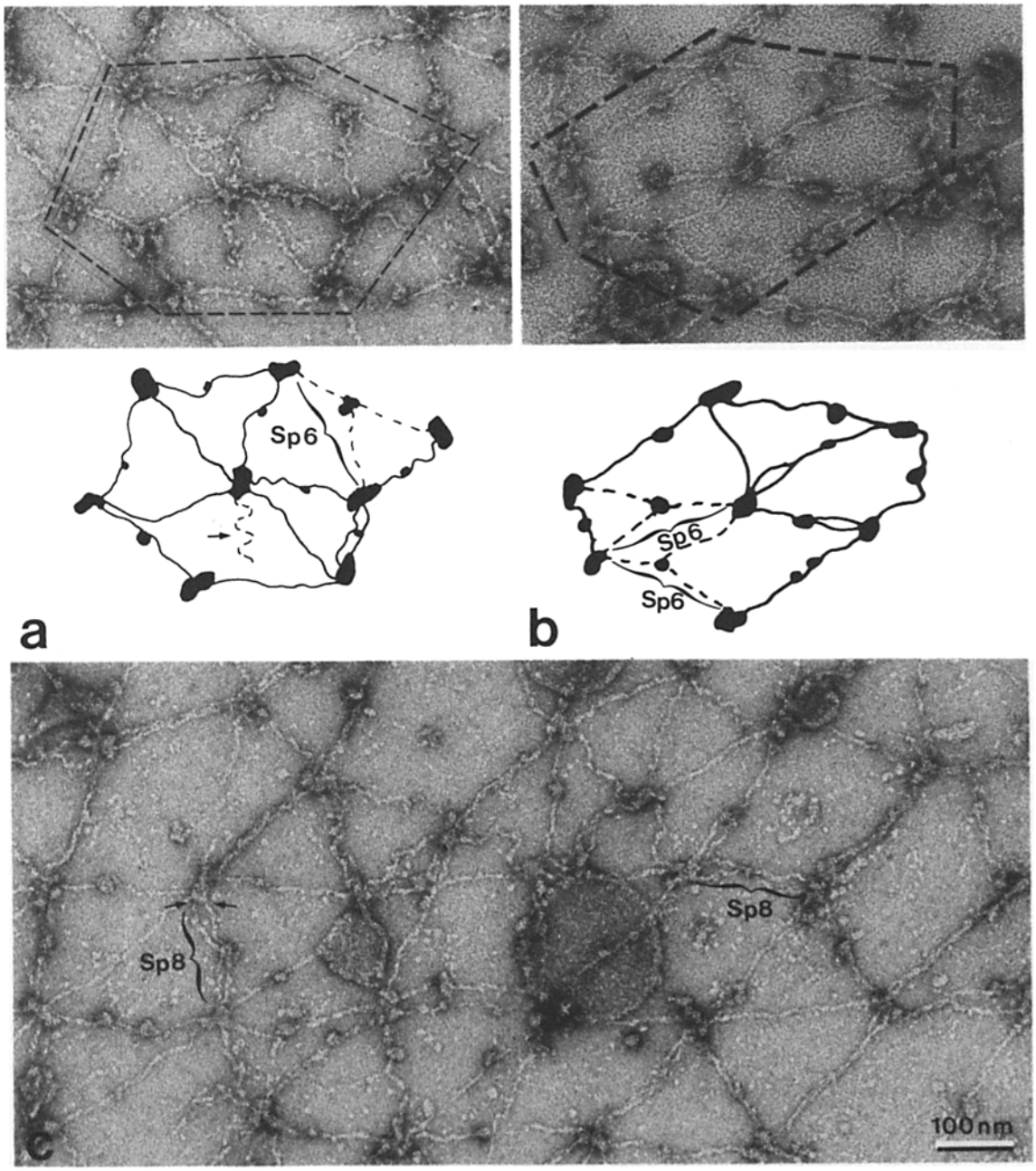

Figure 6. Junctional complexes of F-actin cross-linked by three- and four-armed spectrin molecules. (*a*) Three-armed spectrin molecules (*dotted line*, Y-shaped structure, *Sp6*) cross-linking three junctional complexes in the skeleton. Arrow indicates a spectrin tetramer with one end detached from the junctional complex. (*b*) Two three-armed spectrin molecules cross-linking a total of four junctional complexes in the skeleton. (*c*) Four-armed spectrin molecules (*Sp8*). In the left four-armed spectrin molecule, the binding of two adjacent arms of spectrin to separate sites of the same junctional complex (*arrows*) can be seen.

ments without the attached 9–12-nm globules at the ankyrin binding sites (Fig. 8 *b*). These data confirm a recent observation by Shen et al. (35) and suggest that the 9–12-nm globules in the native skeleton represent ankyrin or ankyrin–band 3 complexes.

Spectrin Tetramer to Dimer Dissociation in Normal Membrane Skeletons

We have previously shown that incubation of normal erythrocyte ghosts at 37°C under hypotonic conditions transformed some of the spectrin tetramers into dimers and reduced the

Figure 5. Double-layered spread membrane skeletons. Spectrin filaments of the bottom skeletal layer are crossed over by spectrin filaments of the upper skeletal layer. Overlapping of the two skeletal layers is also indicated by the regions of residual membrane components (*asterisks*) not extracted by Triton X-100.

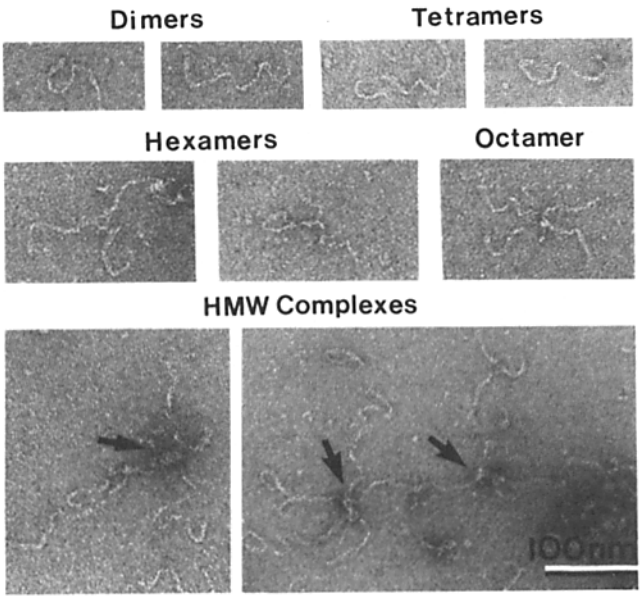

Figure 7. Electron micrographs of negatively stained spectrin in the 0°C-crude spectrin extract. Crude spectrin was extracted from normal red cell ghosts by incubation at low ionic strength (0.1 mM NaPi, pH 8) at 0°C for 24 h. The extract was examined by negative staining electron microscopy as described in Fig. 1. Spectrin dimers and tetramers appear as long convoluted filaments, 100 and 200 nm long, respectively. Spectrin hexamers and octamers appear as polyskelion structures similar to that shown by low-angle rotary shadowing techniques (21). The spectrin-actin-band 4.1 (HMW) complexes contain a structure, as indicated by arrows, similar to the short F-actin found in the spread skeleton. An example of two short F-actins cross-linked by a spectrin tetramer is shown in the lower right-hand micrograph. Note that there is no evidence of splitting of α- and β-chains in the negatively stained spectrin.

mechanical stability of membrane skeletons (22). In the present study, we explored the possible alterations of membrane skeletal assembly related to this spectrin tetramer to dimer dissociation. After incubating ghosts in 5 mM NaPi, pH 7.4, containing 15 mM NaCl at 37°C, some of the spectrin tetramers (50%) were dissociated into dimers as demonstrated by nondenaturing gel analysis of the spectrin species in the 0°C low-salt membrane extract (Fig. 9 *a*). Ultrastructural studies of these spectrin dimer-enriched membrane skeletons revealed a gross disruption of the hexagonal lattice characterized by fewer cross-bridges and large spaces (Fig. 9 *b*). In addition, it appeared that more proteins, presumably the dissociated spectrin dimers, were aggregated onto the junctional complexes in these disrupted skeletal meshworks.

Discussion

The present study suggests that the spread membrane skeleton of the normal erythrocyte is organized into a hexagonal lattice of junctional F-actin complexes cross-linked by spectrin tetramers and, possibly, other oligomers. Some of the junctional complexes are arranged in the form of pentagons (3%) and septagons (8%). Extensive regions of the erythrocyte membrane skeleton are reproducibly visualized, which demonstrates for the first time that the hexagonal-pentagonal arrays seen by others (5, 35) are a regular repeating pattern of the entire membrane skeleton.

The membrane skeleton images presented in this paper argue against the existence of extensive regions of oligomeric spectrin complexes not associated with periodic actin-band 4.1 junctions as previously proposed by others (25, 26, 28, 29). We did not detect any large spectrin oligomers (e.g., 20 units) formed by head to head association of spectrin dimers

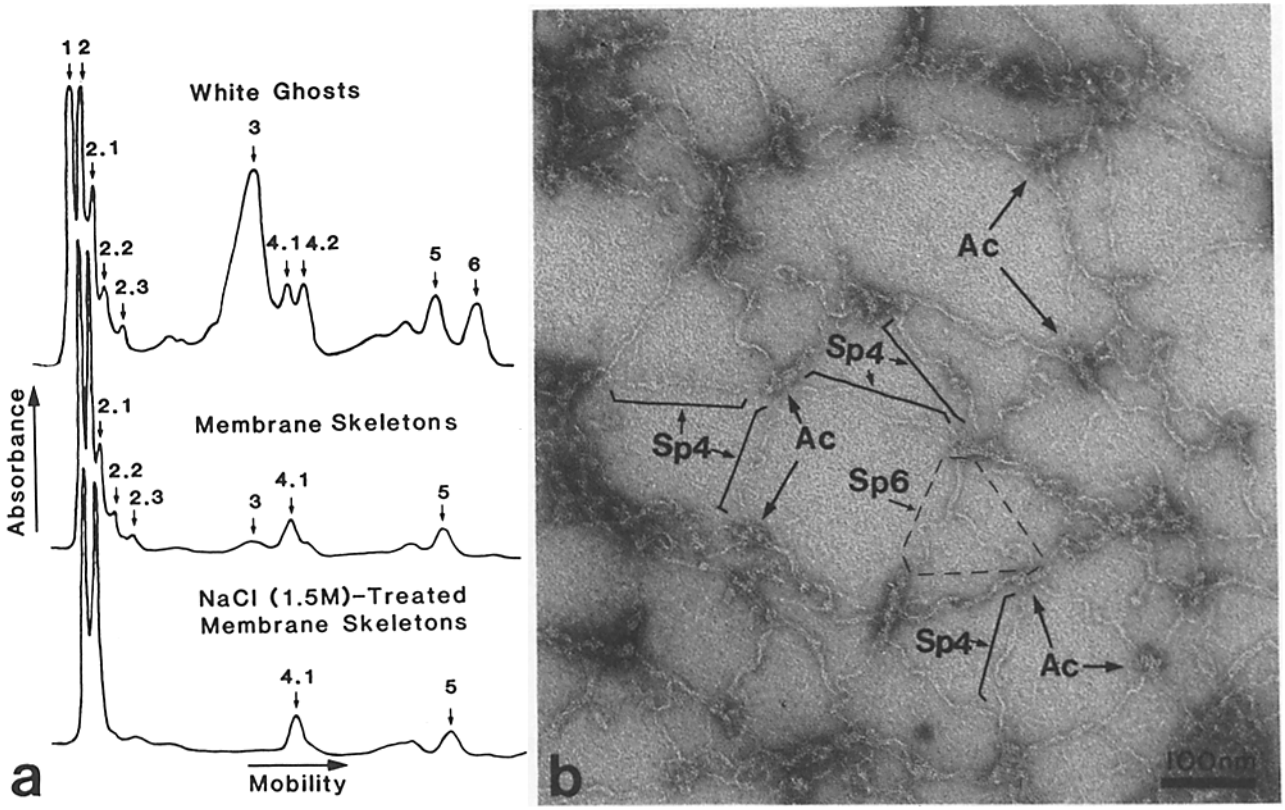

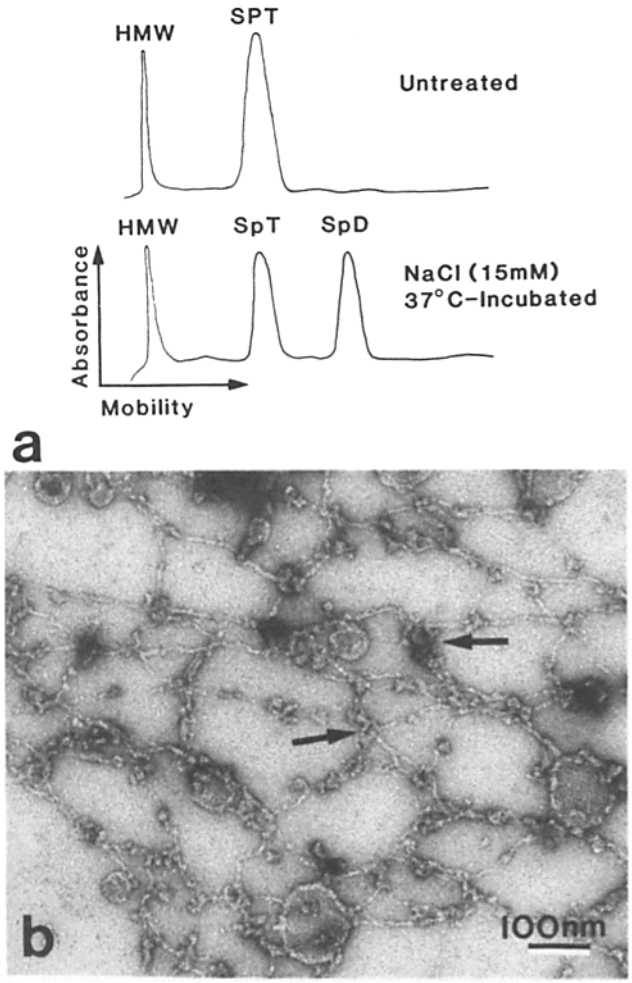

Figure 9. Spectrin dimer-enriched red cell membrane skeletons. To induce a partial dissociation of spectrin tetramers into dimers, ghosts from normal red cells were incubated hypotonically at 37°C for 15 min in 5 mM NaPi (pH 7.4) containing 15 mM NaCl. (*a*) Ghosts were washed and extracted in low-salt buffer at 0°C. The distribution of spectrin species in the extract was analyzed by nondenaturing gel electrophoresis (20). The densitometric scans of the gels indicate that 50% of the spectrin tetramers (SpT) were converted to dimers (SpD). (*b*) Membrane skeletons were prepared from these spectrin dimer-enriched ghosts and examined as described in Fig. 1. Note that the hexagonal lattice is grossly disrupted in the skeleton enriched in spectrin dimers. The broken spectrin filaments tend to aggregate on the adjacent spectrin filament or the junctional complex (*arrows*) during the specimen preparation for electron microscopic examination.

in the spread skeleton. The other possibility that large spectrin oligomers may form by tail to tail self-association, independent of, yet obscured by junctional complexes, is also unlikely. This conclusion is based on several previous observations: (*a*) the α I domain (80,000 mol wt) of spectrin is an effective competitor for spectrin dimer-tetramer-oligomer transformation (29), suggesting that spectrin oligomers in solution are formed by an extension of the same process, i.e., head to head association responsible for the tetramer, (*b*) the tail end of isolated spectrin binds strongly to F-actin in the presence of band 4.1 (7, 8, 9, 44), forming ternary complexes with a morphology similar to the junctional complexes of the spread skeleton, and (*c*) the association of spectrin with short F-actin in membrane skeletal fragments can be displaced by the S1 fragment of heavy meromyosin (34), suggesting that spectrin binds to a specific site on the actin molecule. Although a high concentration of spectrin in solution favors the formation of multimeric spectrin complexes, it is possible that high in situ concentrations of ankyrin, actin, band 4.1, and band 4.9 in the membrane greatly constrain spectrin and limit its ability to self-associate. The distribution of spectrin species in the membrane in situ has previously been measured indirectly in the crude spectrin extract eluted from the membrane at 0°C (21). This is based on the assumption that the native spectrin species in the membrane is kinetically trapped in its oligomeric state at 0°C during the extraction and subsequent in vitro analysis. This biochemical approach revealed that spectrin tetramers, hexamers, and medium-sized oligomers are the prominent species in the membrane. The detection in the present study of two- to four-armed spectrin structures cross-linking adjacent junctional complexes of the spread skeleton is compatible with the presence of spectrin tetramers and medium-sized oligomers, but not large spectrin complexes, in the native erythrocyte membrane.

Based on the presence of a hexagonal lattice in the skeleton and the known stoichiometry of one spectrin dimer to 2.5 actin monomers in erythrocyte membranes (13), the data suggest that short F-actin in the junctional complexes may contain about 15 actin monomers with a calculated dimension of 41 nm long. This value is consistent with that of 10–18 protomers determined by the cytochalasin binding study (4, 18, 19, 31). However, the size and shape of the junctional complexes in the spread skeleton are somewhat heterogeneous; the width varies from 9 to 16 nm and the length varies from ~38 to 50 nm. It is possible that membrane lipids and nonskeletal proteins are not completely extracted from ghosts by Triton X-100 or that the junctional complexes of the Triton shells are still decorated with various nonessential membrane components. Recently, we have detected the presence of large junctional complexes (80–140 nm in diameter) in the membrane skeleton prepared from reticulocytes of acetylphenylhydrazine-treated rats, but not from untreated control animals (Liu et al., unpublished observation). It is possible that junctional complexes of actin, band 4.1, and actin-binding proteins such as band 4.9, tropomyosin, and myosin (14, 15, 37, 46) undergo structural remodeling and size reduction during reticulocyte–erythrocyte maturation.

Finally, our studies confirmed that the 9–12-nm globular

Figure 8. Ankyrin-depleted red cell membrane skeletons. Triton (2.0%)-treated membrane ghosts (i.e., membrane skeletons) were centrifuged through a 10% sucrose cushion containing 5 mM NaPi (pH 7) with and without 1.5 M NaCl. (*a*) Protein composition of skeletons analyzed by SDS PAGE. Hypotonically prepared membrane skeletons retain spectrin, actin, band 4.1, 60% of the ankyrin, and 10% of band 3. After a subsequent high-salt treatment, most of the ankyrin and band 3 are removed from the skeleton. (*b*) Ultrastructure of the ankyrin-depleted membrane skeletons. The high-salt treated skeleton is somewhat aggregated but still contains recognizable junctional complexes that are linked by bare spectrin filaments, i.e., without the attached 9–12-nm globules.

structures at the spectrin–ankyrin binding sites in the skeleton could be removed by high salt treatment (Fig. 8 *b*). Protein composition analysis revealed that ankyrin and residual band 3 were extracted from the skeleton under these conditions. This selective extraction thus provides independent evidence for the lumps others have visualized and tentatively identified as "occupied" ankyrin binding sites (5, 35).

We thank Loretta Wencis for manuscript preparation and Mia Thurlow for her artwork. We acknowledge the Robert J. Kleberg, Jr. and Helen C. Kleberg Foundation for its generous donation of equipment funds to the Electron Microscopy Facility at St. Elizabeth's Hospital of Boston.

This work was supported by grants from the National Institutes of Health (HL-27215, HL-37462, and HL-30269).

Received for publication 22 September 1986, and in revised form 17 November 1986.

References

1. Atkinson, M. A., J. S. Morrow, and V. T. Marchesi. 1982. The polymeric state of actin in the human erythrocyte cytoskeleton. *J. Cell. Biochem.* 18:493–505.

2. Branton, D., C. M. Cohen, and J. Tyler. 1981. Interaction of cytoskeletal proteins on the human erythrocyte membrane. *Cell.* 24:24–32.

3. Brenner, S. L., and E. D. Korn. 1980. Spectrin-actin interaction: phosphorylated and dephosphorylated spectrin tetramer crosslink F-actin. *J. Biol. Chem.* 254:8620–8627.

4. Brenner, S. L., and E. D. Korn. 1980. Spectrin-actin complex isolated from sheep erythrocytes accelerates actin polymerization by simple nucleation: evidence for oligomeric actin in the erythrocyte cytoskeleton. *J. Biol. Chem.* 255:1670–1676.

5. Byers, T. J., and D. Branton. 1985. Visualization of the protein associations in the erythrocyte membrane skeleton. *Proc. Natl. Acad. Sci. USA.* 82: 6153–6157.

6. Cohen, C. M. 1983. The molecular organization of red cell membrane skeleton. *Semin. Hematol.* 20:141–158.

7. Cohen, C. M., and S. F. Foley. 1980. Spectrin-dependent and -independent association of F-actin with the erythrocyte membrane. *J. Cell Biol.* 86: 694–698.

8. Cohen, C. M., and S. F. Foley. 1982. The role of band 4.1 in the association of actin with erythrocyte membranes. *Biochim. Biophys. Acta.* 688:691–701.

9. Cohen, C. M., J. M. Tyler, and D. Branton. 1980. Spectrin-actin associations studied by electron microscopy of shadowed preparations. *Cell.* 21: 875–883.

10. Craig, R., A. G. Szent-Gyorgyi, L. Beese, P. Flicker, P. Vibert, and C. Cohen. 1980. Electron microscopy of thin filaments decorated with a Ca^{2+}-regulated myosin. *J. Mol. Biol.* 140:35–55.

11. Dodge, J. T., C. Mitchell, and D. J. Hanahan. 1963. The preparation and chemical characteristics of hemoglobin free ghosts of human erythrocytes. *Arch. Biochem. Biophys.* 100:119–130.

12. Espevik, T., and A. Elgsaeter. 1981. A freeze-etch electron microscopic study of liquid propane jet-frozen human erythrocyte membranes. *J. Micros. (Oxf.).* 122:159–163.

13. Fairbanks, G., T. L. Steck, and D. F. H. Wallach. 1971. Electrophoretic analysis of the major polypeptide of the human erythrocyte membrane. *Biochemistry.* 10:2606–2617.

14. Fowler, V. M., and V. Bennet. 1983. Erythrocyte membrane tropomyosin. Purification and properties. *J. Biol. Chem.* 259:5978–5989.

15. Fowler, V. M., J. Q. Davies, and V. Bennet. 1985. Human erythrocyte myosin: identification and purification. *J. Cell Biol.* 100:47–55.

16. Fowler, V. M., and D. L. Taylor. 1980. Spectrin plus band 4.1 crosslink actin. *J. Cell Biol.* 85:361–376.

17. Hainsfeld, J. F., and T. L. Steck. 1977. The sub-membrane reticulum of the human erythrocyte: a scanning electron microscope study. *J. Supramol. Struct.* 6:301–311.

18. Lin, D. C. 1981. Spectrin-4.1-actin complex of the human erythrocyte: molecular basis of its ability to bind cytochalasins with high-affinity, and to accelerate actin polymerization in vitro. *J. Supramol. Struct. Cell. Biochem.* 15: 129–138.

19. Lin, D. C., and S. Lin. 1979. Actin polymerization induced by a motility related high affinity binding complex from human erythrocyte membranes. *Proc. Natl. Acad. Sci. USA.* 76:2345–2349.

20. Liu, S. C., J. Palek, J. Prchal, and R. P. Castleberry. 1981. Altered spectrin dimer–dimer association and instability of erythrocyte membrane skeletons in hereditary pyropoikilocytosis. *J. Clin. Invest.* 68:597–605.

21. Liu, S. C., P. Windisch, S. Kim, and J. Palek. 1984. Oligomeric states of spectrin in normal erythrocyte membranes: biochemical and electron microscopic studies. *Cell.* 37:587–594.

22. Liu, S. C., and J. Palek. 1980. Spectrin tetramer-dimer equilibrium and the stability of erythrocyte skeletons. *Nature (Lond.).* 285:586–588.

23. Liu, S. C., and J. Palek. 1984. Hemoglobin enhances the self-association of spectrin heterodimers in human erythrocyte. *J. Biol. Chem.* 259:11556–11562.

24. Liu, S. C., L. H. Derick, and J. Palek. 1985. High resolution electron microscopic study of normal and abnormal RBC membrane skeletons. *Blood.* 66:35*a*. (Abstr.)

25. Marchesi, V. T. 1983. The red cell membrane skeleton: recent progress. *Blood.* 61:1–11.

26. Marchesi, V. T. 1985. Stabilizing infrastructure of cell membranes. *Annu. Rev. Cell Biol.* 1:531–561.

27. Mohandas, N., J. Wyatt, S. F. Mel, M. E. Rossi, and S. B. Shohet. 1982. Lipid translocation across the human erythrocyte membrane. *J. Biol. Chem.* 257:6537–6543.

28. Morrow, J. S., and V. T. Marchesi. 1981. Self-assembly of spectrin oligomers in vitro: a basis for a dynamic cytoskeleton. *J. Cell Biol.* 88:463–468.

29. Morrow, J. S., W. B. Haigh Jr., and V. T. Marchesi. 1981. Spectrin oligomers: a structural feature of the erythrocyte cytoskeleton. *J. Supramol. Struct. Cell. Biochem.* 17:275–287.

30. Nermut, M. V. 1981. Visualization of the membrane skeleton in human erythrocytes by freeze-etching. *Eur. J. Cell Biol.* 25:265–271.

31. Pinder, J. C., and W. B. Gratzer. 1983. Structure and dynamic states of actin in the erythrocyte. *J. Cell Biol.* 96:768–775.

32. Sheetz, M. P. 1979. Integral membrane protein interaction with triton cytoskeletons of erythrocytes. *Biochim. Biophys. Acta.* 557:122–134.

33. Sheetz, M. P., and D. Sawyer. 1978. Triton shells of intact erythrocytes. *J. Supramol. Struct.* 8:399–412.

34. Shen, B. W., R. Josephs, and T. L. Steck. 1984. Ultrastructure of unit fragments of the skeleton of the human erythrocyte membrane. *J. Cell Biol.* 99:810–821.

35. Shen, B. W., R. Josephs, and T. L. Steck. 1986. Ultrastructure of the intact skeleton of the human erythrocyte membrane. *J. Cell Biol.* 102:997–1006.

36. Shotton, M. D., B. E. Burke, and D. Branton. 1979. The molecular structure of human erythrocyte spectrin. Biophysical and electron microscopic studies. *J. Mol. Biol.* 131:303–329.

37. Siegel, D. L., and D. Branton. 1985. Partial purification and characterization of an actin-bundling protein, band 4.9, from human erythrocytes. *J. Cell Biol.* 100:775–785.

38. Smith, P. R. 1979. A trough designed to facilitate the coating of electron microscope grids. *Sci. Tools.* 26:51–52.

39. Timme, A. H. 1981. The ultrastructure of the erythrocyte cytoskeleton at neutral and reduced pH. *J. Ultrastruct. Res.* 77:199–209.

40. Tsukita, S., S. Tsukita, and H. Ishikawa. 1980. Cytoskeletal network underlying the human erythrocyte membrane. Thin section electron microscopy. *J. Cell Biol.* 85:567–576.

41. Tsukita, S., S. Tsukita, and H. Ishikawa. 1984. Bidirectional polymerization of G-actin on the human erythrocyte membrane. *J. Cell Biol.* 98:1102–1110.

42. Tyler, J. M., and D. Branton. 1980. Rotary shadowing of extended molecules dried from glycerol. *J. Ultrastruct. Res.* 71:95–102.

43. Tyler, J. M., B. N. Reinhardt, and D. Branton. 1980. Associations of erythrocyte membrane proteins: binding of purified bands 2.1 and 4.1 to spectrin. *J. Biol. Chem.* 255:7034–7039.

44. Ungewickell, E., P. M. Bennet, R. Calvert, V. Ohanian, and W. B. Gratzer. 1979. In vitro formation of a complex between cytoskeletal proteins of the human erythrocyte. *Nature (Lond.).* 280:811–814.

45. Ungewickell, E., and W. Gratzer. 1978. Self-association of human spectrin: a thermodynamic and kinetic study. *Eur. J. Biochem.* 88:379–385.

46. Wong, A. J., D. P. Kiehart, and T. D. Pollard. 1985. Myosin from human erythrocytes. *J. Biol. Chem.* 260:46–49.

47. Yu, J., D. A. Fischman, and T. L. Steck. 1973. Selective solubilization of proteins and phospholipids from red blood cell membranes by nonionic detergents. *J. Supramol. Struct.* 1:233–248.